PCCP

Kinetic-energy-based error quantification in Kohn-Sham density functional theory

Journal:	*Physical Chemistry Chemical Physics*
Manuscript ID	CP-ART-08-2019-004595.R2
Article Type:	Paper
Date Submitted by the Author:	19-Nov-2019

Complete List of Authors:	Mostafanejad, Mohammad; Florida State University, Chemistry and Biochemistry Haney, Jess; Florida State University, Chemistry and Biochemistry DePrince, Eugene; Florida State University, Chemistry and Biochemistry;

PCCP

ARTICLE TYPE

Cite this: DOI: 00.0000/xxxxxxxxxx

Kinetic-energy-based error quantification in Kohn-Sham density functional theory†

Mohammad Mostafanejad,[a] Jessica Haney,[a] and A. Eugene DePrince III*[a]

Received Date
Accepted Date

DOI: 00.0000/xxxxxxxxxx

We present a basis-independent metric to assess the quality of the electron density obtained from Kohn-Sham (KS) density functional theory (DFT). Given an exact reference density, Levy's constrained search (CS) formalism yields the exact non-interacting kinetic energy. The difference between this value and the kinetic energy obtained from a KSDFT procedure employing an approximate density functional serves as a measure of the density-driven error in the KS solution, which complements other error analyses based solely on the density. The CS also has the nice feature that it provides an estimate of the exact kinetic correlation energy as a byproduct of the procedure.

1 Introduction

Since the pioneering works of Hohenberg, Kohn, and Sham,[1,2] the Kohn-Sham (KS) formulation of density functional theory (DFT), having been successfully applied to a variety of molecular systems,[3–6] has become a routine and seemingly indispensible component of modern chemical research. Despite its well-documented successes, many challenges have yet to be fully resolved,[7] and peculiar aspects of the practical realization of KSDFT continue to emerge.[8] Further, some have even argued that DFT has lost its way,[9] relying too heavily on empirical density functionals that might lead to inaccurate densities, despite accurate predictions of ground state energies. This controversial suggestion ignited a rich debate[10–18] regarding the subjectivity of density error quantification in KSDFT, as well as the chemical significance of such errors. The controversial aspects of Ref. 9 have been examined by multiple groups,[13,19,20] with Nagy[17] and Burke[18] and their coworkers, in particular, raising two fundamental concerns regarding the relevance of the central conclusions of that work: (i) the inaccessibility of the exact density through KSDFT in finite basis and (ii) the lack of a universal mathematical metric for the density error. These issues are the focus of the present study.

The formal issue raised in Ref. 17 pertains to a key assumption in KSDFT: that both the physical and non-interacting systems *must* share the same electron density function.[2] While this assertion is sound in the integro-

[a] *Department of Chemistry and Biochemistry, Florida State University, Tallahassee, FL 32306-4390; E-mail: adeprince@fsu.edu*

† Electronic Supplementary Information (ESI) available: [details of any supplementary information available should be included here]. See DOI: 00.0000/00000000.

‡ Additional footnotes to the title and authors can be included *e.g.* 'Present address:' or 'These authors contributed equally to this work' as above using the symbols: ‡, §, and ¶. Please place the appropriate symbol next to the author's name and include a `\footnotetext` entry in the the correct place in the list.

differential representation of KSDFT or within a complete one-electron basis set, it is invalid in a finite basis, as one cannot, in this case, represent the exact density with a single KS determinant.[17] In other words, in a finite basis set, an idempotent KS density matrix and the exact, correlated density matrix can never map onto the same electron density function. Nevertheless, building upon numerous studies of the subtleties of DFT,[21–27] the Hohenberg-Kohn theorem has been re-stated and extended[28] to finite one-particle subspaces. Note that this generalization necessitates additional stability constraints[29] that are typically ignored in practical calculations.

The second issue, raised in Ref. 18, is the lack of a universal mathematical measure of the accuracy of an approximate density, $\tilde{n}(\mathbf{r})$. The authors of that work suggest that, no matter how reasonable a density-error metric may be, the conclusions drawn regarding the accuracy of $\tilde{n}(\mathbf{r})$ will depend on the precise definition of that metric. The variational principle is the most natural and well-defined tool for error quantification in KSDFT; as such, the total energy functional $E[\cdot]$ was introduced as the ideal metric for the error in the approximate density.[18] In this way, the energy error can be partitioned into that resulting from the use of an approximate density functional (*i.e.*, functional-driven error) and that resulting from the error in the density itself (*i.e.*, density-driven error). In reality, however, these sources of error are strongly entangled and differentiating them is non-trivial.[18,30,31]

In this work, we aim to partially resolves the complexities outlined above. We propose an error analysis based on an *exact* density functional, which allows for an unambiguous definition of the density-driven error. To this end, we adopt Levy's constrained search (CS)[32] within the framework of the inverse KSDFT problem.[33–62] A rich literature explores various aspects of the inverse KSDFT problem, to which we refer the interested reader. In the CS procedure described below, we use the non-interacting kinetic energy functional, $T_s[\cdot]$, to construct a non-interacting v-representable density that *can* be arbitrarily close to a given reference density, $n(\mathbf{r})$;[23] this target density could be taken from *ab initio* calculations or experimental methods such as single-crystal X-ray diffraction and spectroscopy.[63–68] The emphasis on "can" reflects the fact that the non-interacting density cannot exactly reproduce a correlated one if the non-interacting density is derived from a determinant of orbitals expanded within a finite basis set. Hence, within a finite basis, the approximate density, $\tilde{n}(\mathbf{r})$, identified through the CS represents the best-possible KS density. The difference between the non-interacting kinetic energy for $\tilde{n}(\mathbf{r})$ and that for some other approximate KS density can be thought of as a purely density-driven error, as it is defined using an *exact* density functional. Further, because this error is defined relative to the best possible KS density matrix, which is idempotent, the metric implicitly accounts for finite-basis issues regarding the representability of the exact density. Given that the exact density and kinetic energy are required inputs for this procedure, the CS also provides an estimate of the kinetic correlation energy, $T_c[n(\mathbf{r})]$, as a byproduct.

This manuscript is organized as follows: Section 2 details the theory underlying the CS and the kinetic-energy-based density error metric. The details of our computations are then described in Sec. 3. In Sec. 4, the CS procedure is applied to the case of molecular nitrogen within several basis sets to demonstrate that the finite nature of the basis does not preclude the existence of highly accurate non-interacting densities. We then apply the kinetic-energy-based density error metric to molecular test set taken from Ref. 12 to rank the performance of some popular approximate density functionals, and we compare our rankings to those obtained with three density-based metrics.

2 Theory

2.1 Constrained search Kohn-Sham density functional theory

According to van Leeuwen's theorem,[23] for a given ensemble v-representable density, we can define a KS procedure that yields a non-interacting ensemble v-representable density with arbitrary accuracy. Based on this idea, we adopt Levy's CS approach[32] which defines the non-interacting KS kinetic energy density functional as

$$T_s[\tilde{n}(\mathbf{r})] := \min_{\Phi\to\tilde{n}} \langle\Phi|\hat{T}|\Phi\rangle \tag{1}$$

where $\hat{T} = -\frac{1}{2}\nabla^2$ denotes the kinetic energy operator, and $\tilde{n}(\mathbf{r})$ is the trial density function. The CS defined by Eq. 1

is performed over all normalized N-electron determinants $|\Phi\rangle$ constructed from orthonormal spin orbitals $\{\psi_i\}$ such that

$$\tilde{n}(\mathbf{r}) = \sum_{i=1}^{N} |\psi_i(\mathbf{r})|^2 \tag{2}$$

and

$$T_s[\tilde{n}(\mathbf{r})] = -\frac{1}{2}\sum_{i=1}^{N} \langle \psi_i|\nabla^2|\psi_i\rangle \tag{3}$$

In order to minimize the difference between the trial density, $\tilde{n}(\mathbf{r})$, and the target density, $n(\mathbf{r})$, we restrict $\tilde{n}(\mathbf{r})$ in the least-squared sense through the constraint

$$\mathscr{C}_1 := \frac{1}{2}\int [n(\mathbf{r}) - \tilde{n}(\mathbf{r})]^2 d\mathbf{r} \tag{4}$$

while preserving the orthogonality of the orbitals:

$$\mathscr{C}_2 := \int \psi_i^*(\mathbf{r})\psi_j(\mathbf{r})\, d\mathbf{r} = \delta_{ij} \tag{5}$$

Note that we employ distinct α- and β-spin orbitals in this formalism, but the density constraint only pertains to the *total* density. We also note that the density constraint is not unique; other forms of the constraint $\mathscr{C}_1$ have also been proposed.[41,42]

We define an augmented Lagrange functional of the density as

$$\begin{aligned}\mathscr{L}[\tilde{n}(\mathbf{r}),\boldsymbol{\lambda},\mu;n(\mathbf{r})] &= T_s[\tilde{n}(\mathbf{r})] - \boldsymbol{\lambda}^{\mathrm{T}}\mathbf{C}[\tilde{n}(\mathbf{r});n(\mathbf{r})] \\ &+ \frac{1}{\mu}||\,\mathbf{C}[\tilde{n}(\mathbf{r});n(\mathbf{r})]\,||^2 \end{aligned} \tag{6}$$

where $\mathbf{C}$ represents a vector comprised of the constraints $\mathscr{C}_1$ and $\mathscr{C}_2$, $\boldsymbol{\lambda}$ represents a vector of Lagrange multipliers associated with these constraints, and μ represents a (non-negative) penalty parameter. The Lagrangian density functional is minimized via a two-step iterative algorithm similar to the first-order semi-definite programming scheme presented in Ref. 69. The first step involves finding the set of orbitals $\{\psi_i^{(k)}(\mathbf{r})\}_{i=1}^{N}$ corresponding to the density function $\tilde{n}^{(k)}(\mathbf{r})$ that minimizes Eq. 6 for a fixed set of Lagrange multipliers $\boldsymbol{\lambda}^{(k)}$ and penalty parameter $\mu^{(k)}$. Here, k is a positive integer denoting the iteration index. In the second step, the Lagrange multipliers are updated by a first-order correction, provided that the maximum absolute error in the constraints has decreased by a factor of four, relative to the maximum absolute error in the constraints in the previous iteration; otherwise, the Lagrange multipliers are not updated:

$$\lambda_I^{(k+1)} = \begin{cases} \lambda_I^{(k)} - \frac{2C_I^{(k+1)}}{\mu^{(k)}}, & \text{if } \frac{\max_I\{|C_I^{(k+1)}|\}}{\max_I\{|C_I^{(k)}|\}} < 0.25 \\ \lambda_I^{(k)}, & \text{otherwise} \end{cases} \tag{7}$$

Here, the index, I, refers to a given constraint. Similarly, in the case that the maximum absolute error in the constraints decreases as described above, the penalty parameter remains fixed; otherwise, it is reduced:

$$\mu^{(k+1)} = \begin{cases} \mu^{(k)}, & \text{if } \frac{\max_I\{|C_I^{(k+1)}|\}}{\max_I\{|C_I^{(k)}|\}} < 0.25 \\ \xi\mu^{(k)}, & \text{otherwise} \end{cases} \tag{8}$$

The parameter ξ is a real random number between $\frac{1}{8}$ and $\frac{1}{12}$. These two steps are repeated until the contraints are satisfied to within a given threshold. Note that the semicolon in Eq. 6 denotes the parametric dependence of the functional on the reference density function, which is held fixed throughout the optimization.

As discussed in Ref. 41, the constraint $\mathscr{C}_1$ can be interpreted as a driving force that directs the trial density $\tilde{n}(\mathbf{r})$ toward the target density $n(\mathbf{r})$ throughout the CS procedure. As demonstrated in the Appendix, in the present case, this driving force can be interpreted as an effective potential, $\tilde{v}_0(\mathbf{r})$, which is defined as

$$\tilde{v}_0(\mathbf{r}) := \frac{\delta\mathscr{C}_1}{\delta\tilde{n}} = n(\mathbf{r}) - \tilde{n}(\mathbf{r}) \tag{9}$$

As the CS proceeds, the difference between the trial and reference densities approaches zero, and the optimal density at $\tilde{n} = n$ has associated with it a set of orbitals that satisfy the KS-like equations

$$[-\frac{1}{2}\nabla^2 + v_{\mathrm{eff}}(\mathbf{r})]\psi_i(\mathbf{r}) = \varepsilon_i\psi_i(\mathbf{r}) \tag{10}$$

The exact definition of the effective potential, $v_{\mathrm{eff}}(\mathbf{r})$, is given in the Appendix.

In comparison with the iterative first-order minimization adopted in this study, the procedure employed by Zhao and Parr[41] and Zhao, Morrison and Parr[42] utilizes a Lagrangian that is not augmented by a penalty parameter. Instead, the optimization is performed via a Tay-

lor expansion of the constraints as a function of the Lagrange multiplier associated with the density constraint and extrapolation techniques. We demonstrate in the Appendix that, in the limit that the constraints are satisfied, the present augmented Lagrangian formalism leads to the KS-like equations defined by Eq. 10, which are similar to those obtained using the formalism of Refs. 41 and 42.

The CS formalism described above is strictly valid in the limit of a complete basis. In this regime, any physical density is representable by a single-determinant of KS orbitals.[17] The present study, however, employs finite sets of basis functions, and, as a result, the constraint $\mathscr{C}_1$ cannot be satisfied to arbitrary accuracy. This limitation slightly changes the mechanism for exiting the iterative two-step procedure outlined above. In this case, the iterations will either terminate if $\mathscr{C}_1$ is satisfied to within a given threshold or if the penalty parameter falls below a preselected value (1×10^{-20}). In Sec. 4, we provide numerical evidence that this basis set effect has little practical impact. That is, the errors displayed by approximate density functions obtained via the CS are far smaller in magnitude than those associated with approximate densities obtained via conventional KSDFT. This observation holds for all approximate density functionals considered in this study.

2.2 A kinetic-energy-based density error metric

Given the exact density, $n(\mathbf{r})$, the correlation energy of the system can be defined, in the DFT sense, as the difference between the exact energy and that of the non-interacting system. Even without knowledge of the exact exchange-correlation functional, the form of the kinetic contribution to the correlation energy, $T_c[n(\mathbf{r})]$, is well defined[43,70]

$$T_c[n(\mathbf{r})] = T[n(\mathbf{r})] - T_s[n(\mathbf{r})] > 0 \tag{11}$$

In a finite basis, however, $T_c[n(\mathbf{r})]$ and $T_s[n(\mathbf{r})]$ are ill defined if $n(\mathbf{r})$ represents the exact density, as this target cannot be exactly reproduced by any trial non-interacting density. We therefore introduce a new functional

$$\Delta[\tilde{n}(\mathbf{r});n(\mathbf{r})] := T[n(\mathbf{r})] - T_s[\tilde{n}(\mathbf{r})] \tag{12}$$

which can serve as a finite-basis approximation to $T_c[n(\mathbf{r})]$ as $\tilde{n}(\mathbf{r})$ approaches $n(\mathbf{r})$; it is clear that $\Delta[\tilde{n}(\mathbf{r});n(\mathbf{r})]$ is asymptotic to the kinetic correlation energy when $\delta n(\mathbf{r}) \to 0$. Thus, a reasonable measure of the error in the approximate density, $\tilde{n}(\mathbf{r})$, is the difference between these two quantities, which reduces to the non-interacting kinetic energy difference calculated for the exact and approximate densities:

$$\begin{aligned}\Upsilon[\tilde{n}(\mathbf{r});n(\mathbf{r})] &:= \Delta[\tilde{n}(\mathbf{r});n(\mathbf{r})] - T_c[n(\mathbf{r})] \\ &= T_s[n(\mathbf{r})] - T_s[\tilde{n}(\mathbf{r})]\end{aligned} \tag{13}$$

For practical calculations in finite basis sets, $T_s[n(\mathbf{r})]$ is ill defined, but $n(\mathbf{r})$ can be replaced by the closest non-interacting density (which is the best possible KS density), which can be obtained via the procedure outlined in the previous subsection.

3 Computational Details

The CS procedure was implemented as a plugin to the Psi4 quantum chemistry package.[71] We considered the molecular set of Mezei *et al.*[12] to evaluate the efficacy of the kinetic-energy-based error quantification. The augmented correlation-consistent polarized-valence quadruple-ζ (aug-cc-pVQZ) basis was used for calculations involving these molecules, the geometries of which were taken from Ref. 12. We also considered the case of molecular nitrogen in three smaller basis sets (6-31G, aug-cc-pVDZ, and aug-cc-pVTZ), and additional computations were performed on atomic/ionic systems within the augmented correlation-consistent polarized weighted-core-valence quintuple-ζ (aug-cc-pwCV5Z) basis set. The reference densities were obtained from coupled-cluster with singles and doubles (CCSD) computations in the relevant basis set. Higher excitations in the reference computations have been considered by Ref. 12, but it has been argued[13] that their presence does not affect the qualitative conclusions about the predicted densities in the atomic and molecular systems considered herein. The only exception is for a study involving the dissociation of molecular nitrogen, for which CCSD would provide inadequate accuracy; in this case, the reference densities were taken from full configuration interaction (FCI) computations performed within the 6-31G basis set. In all computations, densities were represented in real space with Psi4's default Treutler-Lebedev (75,302) grid.

4 Results and Discussion

4.1 Representability of the density in finite basis sets

As argued in Ref. 17, one of the peculiarities of density error quantification in KSDFT is the fact that, in a finite basis set, a KSDFT-derived density cannot reproduce the exact density, or any other correlated density, computed within the same finite basis set. Here, we employ Levy's CS to numerically demonstrate that this formal restriction is practically irrelevant. That is, the best possible KS density matrix, obtained from the CS, is far more accurate than other approximate density matrices derived from conventional KSDFT computations with common density functionals.

Figure 1 depicts errors in DFT-derived densities along the bond axis of molecular nitrogen, as computed in three different basis sets. Approximate densities are taken from the CS and from conventional KSDFT using the PBE,[72] TPSS,[73–75] and B3LYP[76,77] functionals, and the reference density is obtained from CCSD. In each case, the CCSD, CS, and KSDFT calculations were carried out in the same basis set. The CS produces non-interacting densities that are highly accurate in all basis sets. On the other hand, each approximate density functional leads to substantial density errors in the vicinity of the nuclei; these errors can be orders of magnitude larger than those displayed by the "best possible" density (note that the CS density errors in Fig. 1 have been scaled by a factor of 50). For example, within the aug-cc-pVQZ basis set [Fig. 1(c)], the maximum absolute errors displayed by the CS, B3LYP, PBE, and TPSS are 0.002, 0.067, 0.195, and 0.403 a.u., respectively. Hence, in contrast to what is stated in the literature,[17] the CS-derived density can accurately reproduce the exact density within a finite basis set. This observation suggests that the errors in approximate densities obtained via approximate density functionals may have more to do with the approximate nature of the functionals than with the formal issue of the representability of a correlated density within a finite basis set.

4.2 T_s, T_c, and density error quantification

Given an exact reference density, the CS formalism yields not only the exact non-interacting density, but also the exact non-interacting and correlation kinetic energies. In a complete basis set, the functional $\Delta[\tilde{n}(\mathbf{r});n(\mathbf{r})]$ provides

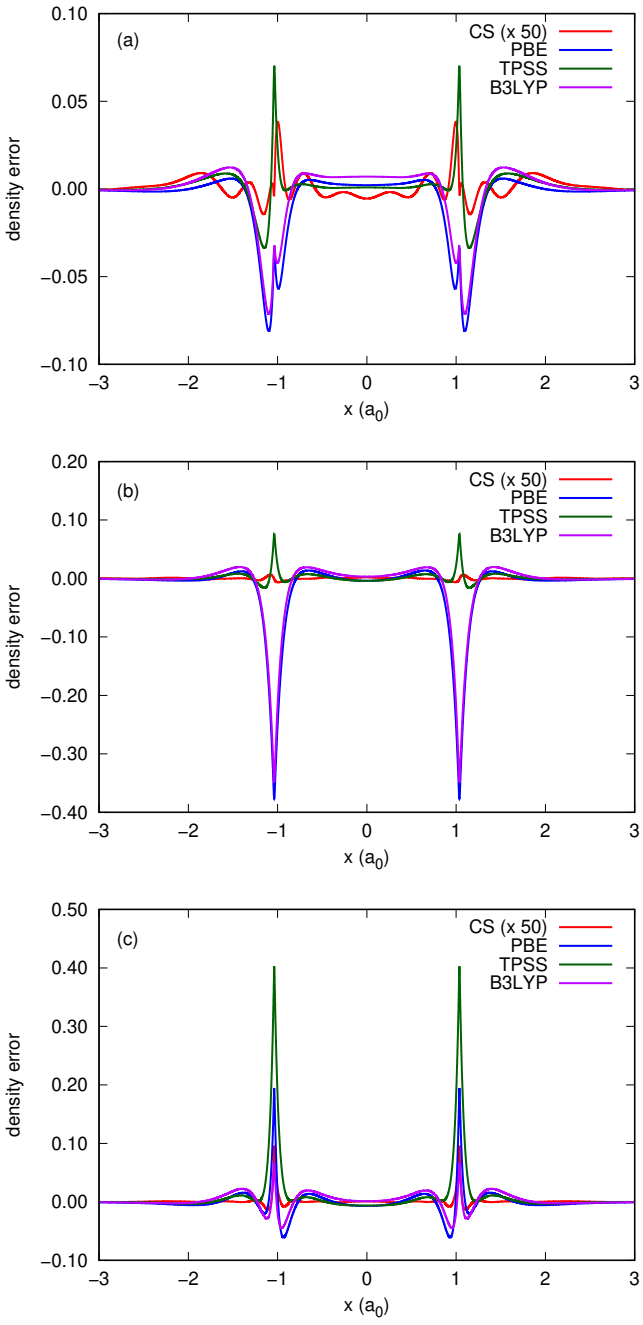

Fig. 1 Errors in densities obtained from various DFT approximations for molecular nitrogen within the (a) aug-cc-pVDZ, (b) aug-cc-pVTZ, and (c) aug-cc-pVQZ basis sets.

an approximation to the kinetic correlation energy, and $\Delta[\tilde{n}(\mathbf{r});n(\mathbf{r})] \sim T_c[n(\mathbf{r})]$ as $\tilde{n}(\mathbf{r}) \to n(\mathbf{r})$. In a finite basis set, $T_c[n(\mathbf{r})]$ is ill defined, but $\Delta[\tilde{n}(\mathbf{r});n(\mathbf{r})]$ can still provide an accurate estimate of $T_c[n(\mathbf{r})]$ if $\tilde{n}(\mathbf{r})$ is the best possible non-interacting approximation to $n(\mathbf{r})$, which can be obtained from the CS. In this section, we evaluate approximate non-interacting and correlation kinetic energies for a variety of atomic and molecular systems, and we demonstrate that these values, obtained within standard finite basis sets, are comparable in quality to "exact" values taken from Ref. 43. We also demonstrate that the approximate non-interacting kinetic energy obtained from the CS can be used to gauge the degree of density-driven error resulting from standard KSDFT with common approximate density functionals.

Table 1 provides numerical estimates of interacting, non-interacting, and correlation kinetic energies for several two-electron atomic ions, as well as literature values for the same ions.[43] In the present computations, the "exact" reference density (denoted n_{CC}) is obtained at the CCSD / aug-cc-pwCV5Z level of theory, and the corresponding (approximate) non-interacting kinetic energy and density (denoted $\tilde{n}_{\mathrm{CS}}$) are obtained from the CS. Literature values for kinetic energies, as well as the density (denoted n), are assumed to be exact. We find that $\Delta[\tilde{n}_{\mathrm{CS}};n_{\mathrm{CC}}]$ reasonably approximates $T_c[n]$ for each ion (to $\approx 0.001\ E_{\mathrm{h}}$). An interesting comparison is that between the non-interacting kinetic energies from Ref. 43 and the present computations; the difference between these values ($\Upsilon[\tilde{n}_{\mathrm{CS}};n] = T_s[n] - T_s[\tilde{n}_{\mathrm{CS}}]$) can be interpreted as a measure of the incompleteness of the one-electron basis employed herein. The numerical values of $\Upsilon[\tilde{n}_{\mathrm{CS}};n]$ are roughly 0.001–0.002 E_{h}, a difference that agrees reasonably well with the difference between the exact literature value for $T_c[n]$ and our estimate for this value, $\Delta[\tilde{n}_{\mathrm{CS}};n_{\mathrm{CC}}]$.

Table 2 provides interacting, non-interacting, and correlation kinetic energies for a set of small molecules. This set was chosen because the systems that comprise it were the subject of a previous study on density error quantification in KSDFT[12]. Estimates of the non-interacting and correlation kinetic energies for these molecules, generated as a byproduct of the CS, are tabulated in Table 2. Total kinetic energies were taken from reference CCSD computations, which were performed within the aug-cc-pVQZ basis set. Non-interacting kinetic energies, T_s, were obtained from the CS procedure, which was also performed within the aug-cc-pVQZ basis set, with the CCSD density serving as the target density. The functional $\Delta[\tilde{n}_{\mathrm{CS}};n_{\mathrm{CC}}]$ then provides an estimate of the kinetic correlation energy. The molecules are arranged in order of increasing numbers of electrons (N), and we note a general increase in the approximate kinetic correlation energy per electron with increasing N.

We now consider the non-interacting kinetic energy as a metric to assess the quality of approximate density functionals and explore its behavior relative to other density error metrics. For this purpose, we first consider the dissociation of molecular nitrogen, as described by FCI and KSDFT (using the B3LYP,[76,77] PBE,[72] and TPSS[73–75] functionals) within the 6-31G basis set. Figure 2 depicts the interacting kinetic energy from FCI and non-interacting kinetic energies, kinetic energy errors, and density errors associated with both restricted [Figs. 2(a), 2(c), and 2(e)] and unrestricted [Fig. 2(b), 2(d), and 2(f)] KSDFT as a function of the N–N distance. Here, "density error" refers to the integral absolute density error per electron ($N^{-1}\int |\tilde{n}_{\mathrm{KS}} - n_{\mathrm{CC}}|\ d\mathbf{r}$). Also included in Figs. 2(a) and 2(b) are the non-interacting kinetic energies generated via the CS procedure that employed FCI target densities.

First, we note that the non-interacting kinetic energies generated via the CS agree reasonably well with the interacting kinetic energies from FCI over the entire range of bond lengths considered, despite the strongly-correlated nature of this problem and the extremely small basis set utilized in the study. Small deviations between the FCI and CS curves can be attributed to both a lack of kinetic correlation energy in the CS curves and, to a lesser extent, the numerical challenges associated with performing the CS procedure in such a small basis set.

Figures 2(c) and 2(d) provide $\Upsilon[\tilde{n}_{\mathrm{KS}};\tilde{n}_{\mathrm{CS}}]$ values for restricted and unrestricted KSDFT, respectively. Non-interacting kinetic energies from restricted calculations deviate significantly from those obtained via the CS, while the kinetic energies obtained from unrestricted calculations are in much better agreement with the CS values, at least beyond the Coulson-Fischer point. If $\Upsilon[\tilde{n}_{\mathrm{KS}};\tilde{n}_{\mathrm{CS}}]$ is used as a measure of the quality of the solution, unre-

Table 1 Interacting, non-interacting, and correlation kinetic energies (E_h) for two-electron atomic ions.

	Ref. 43			this work[a,b]			
	$T_s[n]$	$T[n]$	$T_c[n]$	$T_s[\tilde{n}_{CS}]$	$T[n_{CC}]$	$\Delta[\tilde{n}_{CS};n_{CC}]$	$\Upsilon[\tilde{n}_{CS};n]$
B^{3+}	21.9885	22.0310	0.0424	21.9872	22.0290	0.0417	0.0013
C^{4+}	32.3631	32.4062	0.0432	32.3615	32.4038	0.0423	0.0016
N^{5+}	44.7381	44.7814	0.0434	44.7360	44.7787	0.0427	0.0021
O^{6+}	59.1126	59.1566	0.0440	59.1105	59.1536	0.0431	0.0021
F^{7+}	75.4871	75.5317	0.0446	75.4852	75.5286	0.0434	0.0019

[a] n_{CC} denotes the CCSD / aug-cc-pwCV5Z reference densities employed in this work
[b] $\tilde{n}_{CS}$ denotes the non-interacting density that most closely approximates n_{CC}

Table 2 Interacting, non-interacting, and correlation kinetic energies (E_h) of small molecules calculated within aug-cc-pVQZ basis set.

	$T[n_{CC}]$	$T_s[\tilde{n}_{CS}]$	$\Delta[\tilde{n}_{CS};n_{CC}]$	$\Delta[\tilde{n}_{CS};n_{CC}]/N$
H_2	1.1737	1.1407	0.0330	0.0165
LiH	8.0116	7.9648	0.0468	0.0117
Li_2	14.8678	14.8186	0.0492	0.0082
BH_3	26.5228	26.3893	0.1335	0.0167
H_2O	76.3198	76.0821	0.2376	0.0238
HF	100.3178	100.0655	0.2523	0.0252
LiF	107.2281	106.9580	0.2702	0.0225
CO	113.1188	112.8054	0.3133	0.0224
N_2	109.3504	109.0357	0.3147	0.0225
F_2	200.3795	199.8950	0.4845	0.0269

stricted KSDFT is clearly preferable to restricted KSDFT, and, of the functionals considered, TPSS and B3LYP provide the best results in the dissociation limit, while PBE exhibits slightly higher errors in this regime. An interesting question is whether similar conclusions can be drawn from a purely density-based error metric; it seems that the answer to this questions is that they can be, in part. First, the density error indicates that unrestricted calculations are preferable to restricted ones, in agreement with the $\Upsilon[\tilde{n}_{KS};\tilde{n}_{CS}]$-based analysis. However, the relative rankings of the functionals predicted by $\Upsilon[\tilde{n}_{KS};\tilde{n}_{CS}]$ and the density error are different. For example, beyond the Coulson-Fischer point, the density error predicts that unrestricted PBE is the highest-quality functional and that unrestricted B3LYP performs the worst in this region; the opposite conclusions can be drawn from Fig. 2(d).

In order to fully understand the discrepancy in the density functional rankings inferred from Fig. 2, we apply four size-intensive density-based error metrics and an expanded set of functionals to the molecular test set considered in Ref. 12. Specifically, we consider the mean absolute kinetic energy error per electron,

$$\varepsilon_{KE} := M^{-1} \sum_{i=1}^{M} (N^{-1} |\Upsilon[\tilde{n}_{KS};\tilde{n}_{CS}]|)_i, \tag{14}$$

the mean integral absolute density error per electron,

$$\varepsilon_{D} := M^{-1} \sum_{i=1}^{M} (N^{-1} \int |\tilde{n}_{KS} - n_{CC}| \, d\mathbf{r})_i, \tag{15}$$

the mean integral absolute gradient error per electron,

$$\varepsilon_{G} := M^{-1} \sum_{i=1}^{M} (N^{-1} \int ||\nabla\tilde{n}_{KS}| - |\nabla n_{CC}|| \, d\mathbf{r})_i, \tag{16}$$

and the mean integral absolute Laplacian error per electron,

$$\varepsilon_{L} := M^{-1} \sum_{i=1}^{M} (N^{-1} \int |\nabla^2\tilde{n}_{KS} - \nabla^2 n_{CC}| \, d\mathbf{r})_i. \tag{17}$$

Here, $\tilde{n}_{KS}$ represents the density obtained from a standard KSDFT computation with an approximate density functional, and the sums run over all M systems of the molecular test set. In Fig. 3, these errors are scaled such that the errors associated with the local spin-density approximation (LSDA) are unity. As representative density functionals, we choose several from multiple rungs of Jacob's ladder, including LSDA (SVWN3,[78–80] not pictured in Fig. 3), GGA (PW91,[81] PBE, BP86,[76,82] and

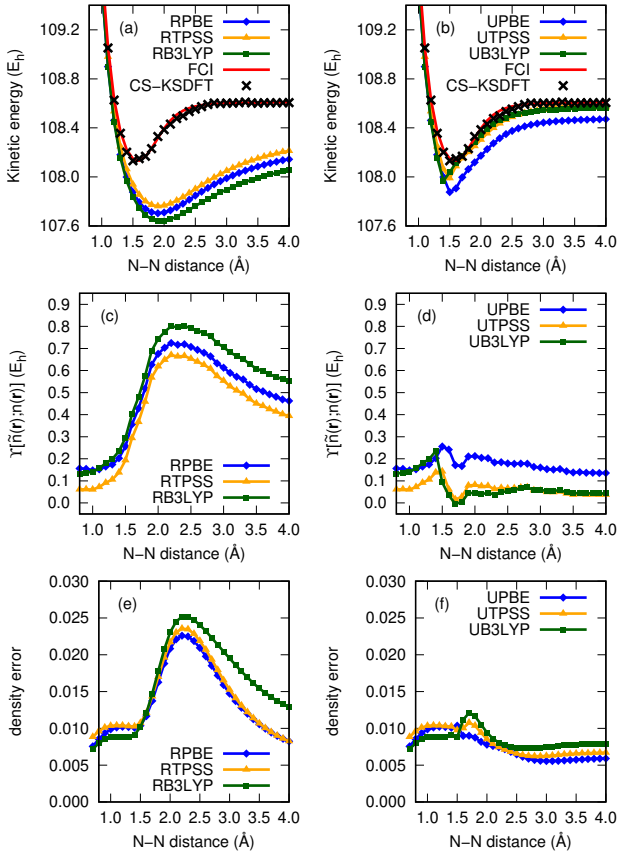

Fig. 2 Interacting and non-interacting kinetic energies for the dissociation of molecular nitrogen computed via FCI and the CS, as compared to non-interacting kinetic energies from (a) restricted and (b) unrestricted KSDFT. Differences between non-intacting kinetic energies from the CS and restricted and unrestricted KSDFT are given in panels (c) and (d), respectively. The integral absolute density errors per electron associated with the restricted and unrestricted KSDFT solutions are given in panels (e) and (f), respectively.

BLYP[76,77]), meta-GGA (TPSS, MS0,[83] SCAN,[84] M06-L,[85] and PKZB[86]), hybrid-(meta)-GGA (M06-2X,[87] B3LYP, SOGGA11-X,[88] TPSSh,[89] and PBE0[90,91]), and range-separated hybrid (CAM-B3LYP,[92] ωPBE,[93] ωB97X,[94] LC-VV10,[95] and HSE06[96,97]) functionals. We also consider the Hartree-Fock (HF) approximation.

Figure 3 illustrates the normalized ε_{D}, ε_{G}, ε_{L}, and $\varepsilon_{\mathrm{KE}}$ errors displayed by each functional listed above when they are applied to the ground electronic states of the molecular set of Mezei *et al.*.[12] First, no matter what metric is utilized, all functionals, including HF, outperform SVWN3 (*i.e.*, all normalized errors are less than unity), which is consistent with the observations of Ref. 12. Second, as Table 3 indicates, we observe improvements in ε_{D}, ε_{G}, ε_{L} errors as the functionals move up Jacob's ladder. On average, hybrid functionals perform better than meta-GGA functionals, which perform better than GGA functionals. We also note that range-separated hybrid functionals, on average, perform similarly to hybrid functionals. The $\varepsilon_{\mathrm{KE}}$ metric, on the other hand, does not display such behavior. All functionals (including HF) perform better than SVWN3, but the average errors corresponding to each class of functional are comparable. Because we interpret $\varepsilon_{\mathrm{KE}}$ as a measure of density-driven error, we conclude that, for the ground states of the molecules that comprise the Mezei set, the density-driven error is comparable for all functional classes (aside from LSDA).

The lack of correlation between $\varepsilon_{\mathrm{KE}}$ and the other error metrics reflects the fact that the latter ones implicitly contain contributions from both density-driven and functional-driven error, while the former measures only density-driven error. This conclusion is supported by an analysis of these same systems using the density-driven error metric of Ref. 18, which is defined as the difference in the total energy (evaluated with an approximate density functional) using the approximate and exact densities. Because the exact density is often inaccessible, the Hartree-Fock density is offered as a proxy for the exact density in that work; accordingly, we define the size-intensive error metric, ΔE_{D}, as

$$\Delta E_{\mathrm{D}} := M^{-1} \sum_{i=1}^{M} [N^{-1}(E_{\mathrm{KS}}[\tilde{n}_{\mathrm{KS}}] - E_{\mathrm{KS}}[\tilde{n}_{\mathrm{HF}}])]_i, \qquad (18)$$

where $E_{\mathrm{KS}}[\cdot]$ represents the total energy evaluated using

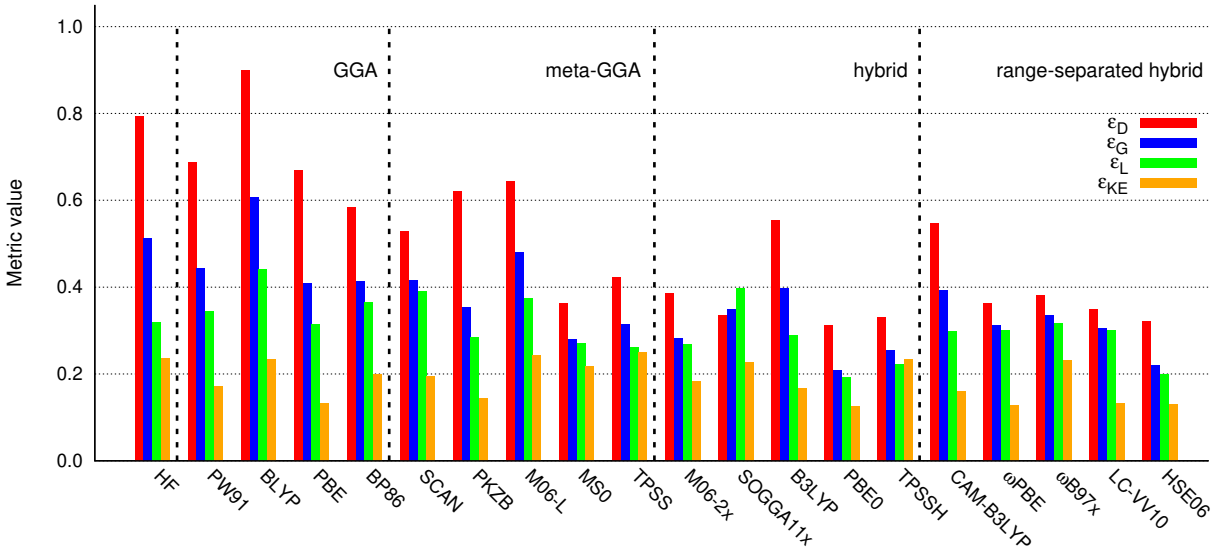

Fig. 3 Density errors for a set of small molecules, as measured by normalized ε_{D}, ε_{G}, ε_{L}, and $\varepsilon_{\mathrm{KE}}$ values.

an approximate density functional, and $\tilde{n}_{\mathrm{HF}}$ represents the HF density. As shown in Table 3, the density-driven error ΔE_{D} does not consistently improve with increasing sophistication of the form of the approximate density functionals, as is observed for ε_{D}, ε_{G}, or ε_{L}. While this behavior is somewhat similar to that observed for $\varepsilon_{\mathrm{KE}}$, the variation in ΔE_{D} accross functional classes is much larger. It is unclear how reliable ΔE_{D} is as a measure of the density-driven error in this case, though, as the HF density hardly approximates the exact density for these systems. Aside from SVWN3 and BLYP, HF presents the largest ε_{D} and ε_{G} errors, and the $\varepsilon_{\mathrm{KE}}$ suggests that the density-driven error in HF is comparable to that of all other functionals considered.

Table 3 Density errors for a set of small molecules, as measured by averaged and normalized ε_{D}, ε_{G}, ε_{L}, $\varepsilon_{\mathrm{KE}}$, and ΔE_{D} values.

functional form	ε_{D}	ε_{G}	ε_{L}	$\varepsilon_{\mathrm{KE}}$	ΔE_{D}
GGA	0.71	0.47	0.37	0.18	0.89
meta-GGA	0.52	0.37	0.32	0.21	0.66
hybrid	0.38	0.30	0.27	0.19	0.78
range-separated	0.39	0.31	0.28	0.16	0.85

5 Conclusions

The controversial work of Medvedev *et al.*[9] has spurred a number of studies on density error quantification in KSDFT. The contentious nature of that paper notwithstanding, it echoed important previous observations[98,99] that a lack of physical insight and unsatisfied universal constraints[100,101] in some popular empirical density functionals can lead to inaccurate densities, despite accurate predictions of ground state energies. Several groups have followed up upon multiple aspects of Ref. 9, including the chemical relevance of the errors analyzed therein,[12] the somewhat subjective nature of density error metrics in general,[18] and the formal issue of the representability of the exact density within a finite basis set.[17]

In this work, we have used Levy's CS within finite basis sets to obtain the best possible KS densities, and we have compared these densities to those generated by common approximate density functionals. We have numerically demonstrated that the best possible non-interacting density is orders of magnitude more accurate than approximate densities obtained with common density functionals. Moreover, we have demonstrated that the non-interacting

kinetic energy that is generated as a byproduct of the CS can be used as a measure of the density-driven error associated with an approximate KSDFT solution. Density error analysis applied to a set of small molecules reveals that the density-driven error is largely independent of the sophistication of the approximate functionals (aside from the lowest rung of Jacob's ladder, the LSDA). Thus, improvements in the quality of the density (as measured by the density itself, the gradient of the density, or the Laplacian of the density) are attributable to a reduction in functional-driven error with increasing sophistication of the functional. Along these lines, these results also suggest that a small density-driven error, as measured by the non-interacting kinetic energy, does not necessarily guarantee a small error in the total energy or other chemical properties, as a good description of T_s could be counterbalanced by a poor exchange-correlation energy; similarly, a large density-driven error does not preclude an accurate description of chemical properties, provided that the exchange-correlation energy compensates for these errors. Lastly, we note that, by considering both spin-restricted and spin-unrestricted KSDFT calculations, one can use the kinetic-energy-based error analysis to isolate contributions to density-driven error stemming from spin restrictions.

A Derivation of Constrained Search Kohn-Sham Density Functional Theory Equations

In this Appendix, we demonstrate that the augmented Lagrangian of Eq. 6 that defines the CS procedure implies a set of KS-like equations, at least in the limit of a complete basis set. We begin by substituting explicit definitions of the least-squared density-difference and orthogonality constraints, $\mathscr{C}_1$, and $\mathscr{C}_2$, respectively, into Eq. 6:

$$\begin{aligned}\mathscr{L}[\tilde{n}(\mathbf{r}),\{\psi_i(\mathbf{r})\},\{\varepsilon_{ij}\},\lambda,\mu;n(\mathbf{r})] &= -\frac{1}{2}\sum_{i=1}^{N}\langle\psi_i|\nabla^2|\psi_i\rangle \\ &-\lambda\left(\frac{1}{2}\int\left[n(\mathbf{r})-\sum_{i=1}^{N}|\psi_i(\mathbf{r})|^2\right]^2 d\mathbf{r}\right)+\frac{1}{4\mu}\left|\int\left[n(\mathbf{r})-\sum_{i=1}^{N}|\psi_i(\mathbf{r})|^2\right]^2 d\mathbf{r}\right|^2 \\ &-\sum_{i=1}^{N}\sum_{j=1}^{N}\varepsilon_{ij}\left(\langle\psi_i|\psi_j\rangle-\delta_{ij}\right)+\frac{1}{\mu}\sum_{i=1}^{N}\sum_{j=1}^{N}|(\langle\psi_i|\psi_j\rangle-\delta_{ij})|^2\end{aligned} \tag{19}$$

Here, ε_{ij} and λ represent undetermined Lagrange multipliers, and μ is the penalty parameter. Allowing linear variation in the finite set of orbitals, $\{\psi_i\}$

$$|\psi\rangle \rightarrow |\psi\rangle + |\delta\psi\rangle \tag{20}$$

the variational principle dictates that[102]

$$\delta\mathscr{L} = 0 \tag{21}$$

Therefore, one can write

$$\begin{aligned}&\delta\left\{-\frac{1}{2}\sum_{i=1}^{N}\langle\psi_i|\nabla^2|\psi_i\rangle-\lambda\left(\frac{1}{2}\int\left[n(\mathbf{r})-\sum_{i=1}^{N}|\psi_i(\mathbf{r})|^2\right]^2 d\mathbf{r}\right)\right. \\ &+\frac{1}{4\mu}\left|\int\left[n(\mathbf{r})-\sum_{i=1}^{N}|\psi_i(\mathbf{r})|^2\right]^2 d\mathbf{r}\right|^2-\sum_{i=1}^{N}\sum_{j=1}^{N}\varepsilon_{ij}\left(\langle\psi_i|\psi_j\rangle-\delta_{ij}\right) \\ &\left.+\frac{1}{\mu}\sum_{i=1}^{N}\sum_{j=1}^{N}|(\langle\psi_i|\psi_j\rangle-\delta_{ij})|^2\right\}=0\end{aligned} \tag{22}$$

in which, the δ, acting on the expression within the curly braces, stands for the functional differential operator (without any indices) and should not be confused with the Kronecker delta tensor δ_{ij}. Performing simple calculus and interchanging dummy indices where necessary, one obtains

$$\left[-\frac{1}{2}\nabla^2+\left(\lambda-\frac{\mathscr{C}_1}{\mu}\right)\tilde{v}_0(\mathbf{r})\right]\psi_i(\mathbf{r})=\sum_{j=1}^{N}\left[\varepsilon_{ij}-\frac{2\mathscr{C}_2}{\mu}\right]\psi_j(\mathbf{r}) \tag{23}$$

where $\tilde{v}_0(\mathbf{r})$ can be interpreted as an the effective potential generated due to the approximate nature of the trial density, $\tilde{n}(\mathbf{r})$ (see Eq. 9 for the definition of $\tilde{v}_0(\mathbf{r})$). Note that the reference density $n(\mathbf{r})$ is fixed during the functional differentiation, as mentioned in Sec. 2. At the stationary point where $\tilde{n}=n$, $\mathscr{C}_1$ and $\mathscr{C}_2$ will be satisfied and vanish. Therefore, while the penalty parameter μ may become small, it remains finite, and the second term on the right-hand side of Eq. 23 ($2\mathscr{C}_2/\mu$) and the third term on the left-hand side of Eq. 23 ($\mathscr{C}_1/\mu$) also vanish. Simultaneously, $\delta n \rightarrow 0$, and one can write

$$v_{\text{eff}}(\mathbf{r}) = \lim_{\tilde{n}\rightarrow n}\left[\left(\lambda-\frac{\mathscr{C}_1}{\mu}\right)\tilde{v}_0(\mathbf{r})\right] \tag{24}$$

which is the definition of the effective potential $v_{\text{eff}}(\mathbf{r})$ mentioned in Eq. 10 of the main text. In this way, Eq.

23 can be recast as

$$\left[-\frac{1}{2}\nabla^2 + v_{\text{eff}}(\mathbf{r})\right]\psi_i(\mathbf{r}) = \varepsilon_{ij}\psi_j(\mathbf{r}) \tag{25}$$

Since Lagrangian functional $\mathscr{L}$ is real and the orthogonality integrals are symmetric, the matrix of Lagrange multipliers $\boldsymbol{\epsilon}$ is Hermitian, *i.e.*,[102]

$$\varepsilon_{ij} = \varepsilon^*_{ji} \tag{26}$$

Hence, there exists a unique unitary transformation matrix $\mathbf{U}$ that diagonalizes the matrix $\boldsymbol{\epsilon}$ to $\boldsymbol{\epsilon}^d$ as

$$\boldsymbol{\epsilon}^d = \mathbf{U}^\dagger \boldsymbol{\epsilon} \mathbf{U} \tag{27}$$

Using the corresponding canonical set of non-interacting KS orbitals, KS-like equations, which are of the same form as those derived in Ref. 41, can be obtained from Eq. 25. Note that this parallel to Ref. 41 is only strictly valid in the complete basis set limit, where we can reasonably expect $\mathscr{C}_1 \to 0$ and $\delta n \to 0$ at convergence.

Conflicts of interest

There are no conflicts to declare.

Acknowledgements

This material is based upon work supported by the Army Research Office Small Business Technology Transfer (STTR) program under Grant No. W911NF-19-C0048 and the National Science Foundation under Grant No. CHE-1554354. Mohammad Mostafanejad was supported by a fellowship from The Molecular Sciences Software Institute under NSF grant ACI-1547580.

Notes and references

1 P. Hohenberg and W. Kohn, *Phys. Rev.*, 1964, **136**, B864–B871.
2 W. Kohn and L. J. Sham, *Phys. Rev.*, 1965, **140**, A1133–A1138.
3 R. G. Parr and W. Yang, *Density-functional theory of atoms and molecules*, Oxford University Press, 1989, p. 333.
4 A. D. Becke, *J. Chem. Phys.*, 2014, **140**, 18A301–18A3018.
5 R. Peverati and D. G. Truhlar, *Philos. Trans. Royal Soc. A*, 2014, **372**, 20120476.
6 N. Mardirossian and M. Head-Gordon, *Mol. Phys.*, 2017, **115**, 2315–2372.
7 A. J. Cohen, P. Mori-Sánchez and W. Yang, *Science*, 2008, **321**, 792–794.
8 A. N. Bootsma and S. Wheeler, *ChemRxiv*, 2019, **preprint**, year.
9 M. G. Medvedev, I. S. Bushmarinov, J. Sun, J. P. Perdew and K. A. Lyssenko, *Science*, 2017, **355**, 49–52.
10 G. Graziano, *Nat. Rev. Chem.*, 2017, **1**, 0019.
11 S. Hammes-Schiffer, *Science*, 2017, **355**, 28–29.
12 P. D. Mezei, G. I. Csonka and M. Kállay, *J. Chem. Theory Comput.*, 2017, **13**, 4753–4764.
13 M. Korth, *Angew. Chem. Int. Ed.*, 2017, **56**, 5396–5398.
14 T. Gould, *J. Chem. Theory Comput.*, 2017, **13**, 2373–2377.
15 K. R. Brorsen, Y. Yang, M. V. Pak and S. Hammes-Schiffer, *J. Phys. Chem. Lett.*, 2017, **8**, 2076–2081.
16 Y. Wang, X. Wang, D. G. Truhlar and X. He, *J. Chem. Theory Comput.*, 2017, **13**, 6068–6077.
17 I. Mayer, I. Pápai, I. Bakó and Á. Nagy, *J. Chem. Theory Comput.*, 2017, **13**, 3961–3963.
18 E. Sim, S. Song and K. Burke, *J. Phys. Chem. Lett.*, 2018, **9**, 6385–6392.
19 K. P. Kepp, *Science*, 2017, **356**, 496.
20 M. G. Medvedev, I. S. Bushmarinov, J. Sun, J. P. Perdew and K. A. Lyssenko, *Science*, 2017, **356**, 496c.
21 E. H. Lieb, *Int. J. Quantum Chem.*, 1983, **24**, 243–277.
22 H. Eschrig, *The Fundamentals of Density Functional Theory*, Teubner, Wiesbaden, 1996, vol. 32.
23 R. van Leeuwen, *Advances in Quantum Chemistry*, 2003, **43**, 25–94.
24 E. V. Ludeña, *J. Mol. Struct. (THEOCHEM)*, 2004, **709**, 25–29.
25 P. W. Ayers and M. Levy, *J. Chem. Sci.*, 2005, **117**, 507–514.
26 A. Görling, *J. Chem. Phys.*, 2005, **123**, 062203.

27 P. W. Ayers, S. Golden and M. Levy, *J. Chem. Phys.*, 2006, **124**, 054101.

28 R. Pino, O. Bokanowski, E. V. Ludeña and R. L. Boada, *Theor. Chem. Acc.*, 2007, **118**, 557–561.

29 R. Pino, O. Bokanowski, E. V. Ludeña and R. L. Boada, *Theor. Chem. Acc.*, 2009, **123**, 189–196.

30 M. C. Kim, E. Sim and K. Burke, *Phys. Rev. Lett.*, 2013, **111**, 073003.

31 M.-C. Kim, E. Sim and K. Burke, *J. Chem. Phys.*, 2014, **140**, 18A528.

32 M. Levy, *Proc. Natl. Acad. Sci. U.S.A*, 1979, **76**, 6062–6065.

33 J. D. Talman and W. F. Shadwick, *Phys. Rev. A*, 1976, **14**, 36–40.

34 A. Nagy and N. H. March, *Phys. Rev. A*, 1989, **39**, 5512–5514.

35 A. Holas and N. H. March, *Phys. Rev. A*, 1991, **44**, 5521–5536.

36 Y. Wang and R. G. Parr, *Phys. Rev. A*, 1993, **47**, R1591–R1593.

37 A. Görling and M. Levy, *Phys. Rev. A*, 1994, **50**, 196–204.

38 A. Görling, *Phys. Rev. B*, 1996, **53**, 7024–7029.

39 R. van Leeuwen and E. J. Baerends, *Phys. Rev. A*, 1994, **49**, 2421–2431.

40 R. G. Parr and S. K. Ghosh, *Phys. Rev. A*, 1995, **51**, 3564–3570.

41 Q. Zhao and R. G. Parr, *J. Chem. Phys.*, 1993, **98**, 543–548.

42 Q. Zhao, R. C. Morrison and R. G. Parr, *Phys. Rev. A*, 1994, **50**, 2138–2142.

43 Q. Zhao and R. G. Parr, *Phys. Rev. A*, 1992, **46**, 2337–2343.

44 R. C. Morrison, *J. Chem. Phys.*, 2002, **117**, 10506–10511.

45 R. C. Morrison and Q. Zhao, *Phys. Rev. A*, 1995, **51**, 1980–1984.

46 J. Garza, J. A. Nichols and D. A. Dixon, *J. Chem. Phys.*, 2000, **113**, 6029.

47 V. N. Staroverov, G. E. Scuseria and E. R. Davidson, *J. Chem. Phys.*, 2006, **124**, 141103–141106.

48 W. Yang and Q. Wu, *Phys. Rev. Lett.*, 2002, **89**, 143002–143006.

49 R. Cuevas-Saavedra, P. W. Ayers and V. N. Staroverov, *J. Chem. Phys.*, 2015, **143**, 244116.

50 E. J. Baerends and O. Gritsenko, *J. Chem. Phys.*, 2016, **145**, 037101.

51 I. G. Ryabinkin, S. V. Kohut, R. Cuevas-Saavedra, P. W. Ayers and V. N. Staroverov, *J. Chem. Phys.*, 2016, **145**, 037102.

52 I. G. Ryabinkin, E. Ospadov and V. N. Staroverov, *J. Chem. Phys.*, 2017, **147**, 164117.

53 I. G. Ryabinkin, S. V. Kohut and V. N. Staroverov, *Phys. Rev. Lett.*, 2015, **115**, 083001.

54 V. E. Ingamells and N. C. Handy, *Chem. Phys. Lett.*, 1996, **248**, 373–378.

55 D. J. Tozer, V. E. Ingamells and N. C. Handy, *J. Chem. Phys.*, 1998, **105**, 9200.

56 D. J. Tozer, N. C. Handy and W. H. Green, *Chem. Phys. Lett.*, 1997, **273**, 183–194.

57 F. Colonna and A. Savin, *J. Chem. Phys.*, 1999, **110**, 2828–2835.

58 Q. Wu and W. Yang, *J. Chem. Phys.*, 2003, **118**, 2498–2509.

59 K. Peirs, D. Van Neck and M. Waroquier, *Phys. Rev. A*, 2003, **67**, 012505.

60 A. M. Teale, S. Coriani and T. Helgaker, *J. Chem. Phys.*, 2009, **130**, 104111.

61 A. M. Teale, S. Coriani and T. Helgaker, *J. Chem. Phys.*, 2010, **132**, 164115.

62 P. W. Ayers, R. C. Morrison and R. G. Parr, *Mol. Phys.*, 2005, **103**, 2061–2072.

63 W. L. Clinton, J. Nakhleh and F. Wunderlich, *Phys. Rev.*, 1969, **177**, 1–6.

64 W. L. Clinton, A. J. Galli and L. J. Massa, *Phys. Rev.*, 1969, **177**, 7–13.

65 W. L. Clinton, G. A. Henderson and J. V. Prestia, *Phys. Rev.*, 1969, **177**, 13–18.

66 W. L. Clinton and G. B. Lamers, *Phys. Rev.*, 1969, **177**, 19–27.

67 W. L. Clinton, A. J. Galli, G. A. Henderson, G. B. Lamers, L. J. Massa and J. Zarur, *Phys. Rev.*, 1969, **177**, 27–33.

68 L. Massa, M. Goldberg, C. Frishberg, R. F. Boehme and S. J. L. Placa, *Phys. Rev. Lett.*, 1985, **55**, 622–

625.
69 D. A. Mazziotti, *ESAIM-Math. Model. Num.*, 2007, **41**, 249–259.
70 M. Levy and J. P. Perdew, *Phys. Rev. A*, 1985, **32**, 2010–2021.
71 R. M. Parrish, L. A. Burns, D. G. A. Smith, A. C. Simmonett, A. E. DePrince, E. G. Hohenstein, U. Bozkaya, A. Y. Sokolov, R. Di Remigio, R. M. Richard, J. F. Gonthier, A. M. James, H. R. McAlexander, A. Kumar, M. Saitow, X. Wang, B. P. Pritchard, P. Verma, H. F. Schaefer, K. Patkowski, R. A. King, E. F. Valeev, F. A. Evangelista, J. M. Turney, T. D. Crawford and C. D. Sherrill, *J. Chem. Theory Comput.*, 2017, **13**, 3185–3197.
72 J. P. Perdew, K. Burke and M. Ernzerhof, *Phys. Rev. Lett.*, 1996, **77**, 3865–3868.
73 J. Tao, J. P. Perdew, V. N. Staroverov and G. E. Scuseria, *Phys. Rev. Lett.*, 2003, **91**, 146401.
74 V. N. Staroverov, G. E. Scuseria, J. Tao and J. P. Perdew, *J. Chem. Phys.*, 2003, **119**, 12129–12137.
75 V. N. Staroverov, G. E. Scuseria, J. Tao and J. P. Perdew, *J. Chem. Phys.*, 2004, **121**, 11507.
76 A. D. Becke, *Phys. Rev. A*, 1988, **38**, 3098–3100.
77 C. Lee, W. Yang and R. G. Parr, *Phys. Rev. B*, 1988, **37**, 785–789.
78 R. Gáspár, *Acta Physica Academiae Scientiarum Hungaricae*, 1974, **35**, 213–218.
79 J. C. Slater, *Phys. Rev.*, 1951, **81**, 385–390.
80 S. H. Vosko, L. Wilk and M. Nusair, *Can. J. Phys.*, 1980, **58**, 1200–1211.
81 J. P. Perdew, J. A. Chevary, S. H. Vosko, K. A. Jackson, M. R. Pederson, D. J. Singh and C. Fiolhais, *Phys. Rev. B*, 1992, **46**, 6671–6687.
82 J. P. Perdew, *Phys. Rev. B*, 1986, **33**, 8822–8824.
83 J. Sun, B. Xiao and A. Ruzsinszky, *J. Chem. Phys.*, 2012, **137**, 051101.
84 J. Sun, A. Ruzsinszky and J. P. Perdew, *Phys. Rev. Lett.*, 2015, **115**, 036402.
85 Y. Zhao and D. G. Truhlar, *J. Chem. Phys.*, 2006, **125**, 194101.
86 J. P. Perdew, S. Kurth, A. c. v. Zupan and P. Blaha, *Phys. Rev. Lett.*, 1999, **82**, 2544–2547.
87 Y. Zhao and D. G. Truhlar, *Theor. Chem. Acc.*, 2008, **120**, 215–241.
88 R. Peverati and D. G. Truhlar, *J. Chem. Phys.*, 2011, **135**, 191102.
89 V. N. Staroverov, G. E. Scuseria, J. Tao and J. P. Perdew, *J. Chem. Phys.*, 2003, **119**, 12129–12137.
90 C. Adamo and V. Barone, *J. Chem. Phys.*, 1999, **110**, 6158–6170.
91 M. Ernzerhof and G. E. Scuseria, *J. Chem. Phys.*, 1999, **110**, 5029–5036.
92 T. Yanai, D. P. Tew and N. C. Handy, *Chem. Phys. Lett.*, 2004, **393**, 51–57.
93 T. M. Henderson, B. G. Janesko and G. E. Scuseria, *J. Chem. Phys.*, 2008, **128**, 194105.
94 J.-D. Chai and M. Head-Gordon, *J. Chem. Phys.*, 2008, **128**, 084106.
95 O. A. Vydrov and T. Van Voorhis, *J. Chem. Phys.*, 2010, **133**, 244103.
96 J. Heyd, G. E. Scuseria and M. Ernzerhof, *J. Chem. Phys.*, 2003, **118**, 8207–8215.
97 A. V. Krukau, O. A. Vydrov, A. F. Izmaylov and G. E. Scuseria, *J. Chem. Phys.*, 2006, **125**, 224106.
98 P. R. Schipper, O. V. Gritsenko and E. J. Baerends, *Phys. Rev. A*, 1998, **57**, 1729–1742.
99 T. Schwabe, *Phys. Chem. Chem. Phys.*, 2014, **16**, 14559–14567.
100 R. J. Bartlett and D. S. Ranasinghe, *Chem. Phys. Lett.*, 2017, **669**, 54–70.
101 D. S. Ranasinghe, A. Perera and R. J. Bartlett, *J. Chem. Phys.*, 2017, **147**, 204103.
102 A. Szabo and N. S. Ostlund, *Modern quantum chemistry : introduction to advanced electronic structure theory*, Dover Publications, 1996, p. 466.

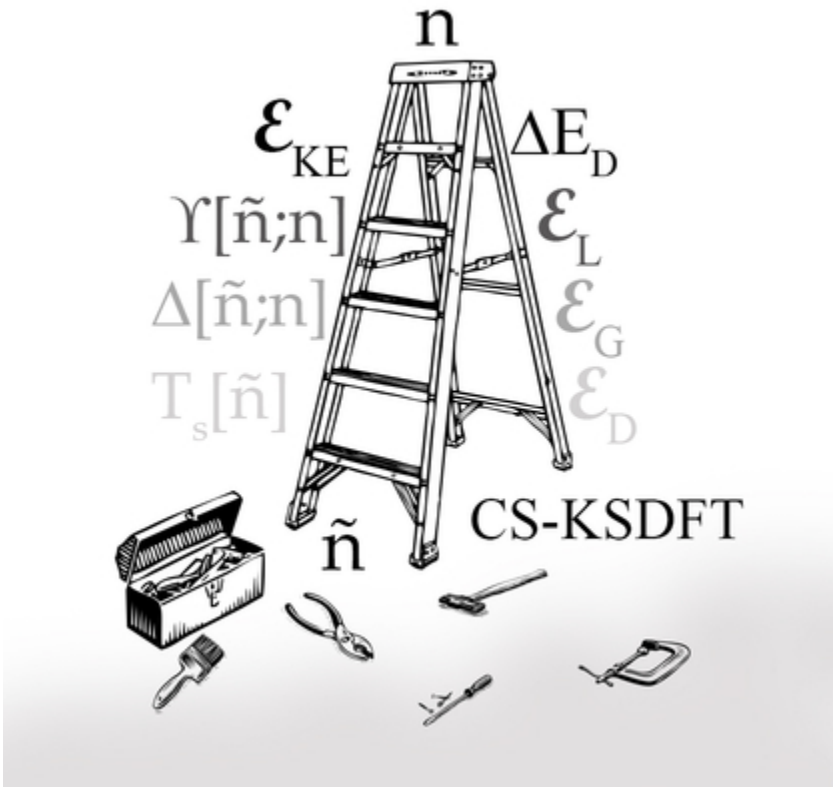

35x34mm (300 x 300 DPI)